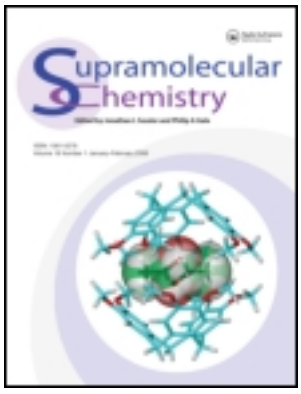

Supramolecular Chemistry
Publication details, including instructions for authors and subscription information:
http://www.tandfonline.com/loi/gsch20

Anthracene-based hetero bisamide chemosensor in fluorescence sensing of monocarboxylates over monocarboxylic acids

Kumaresh Ghosh [a] & Avik Ranjan Sarkar [a]
[a] Department of Chemistry, University of Kalyani, Kalyani, Nadia, 741235, India

Available online: 03 May 2011

To cite this article: Kumaresh Ghosh & Avik Ranjan Sarkar (2011): Anthracene-based hetero bisamide chemosensor in fluorescence sensing of monocarboxylates over monocarboxylic acids, Supramolecular Chemistry, 23:7, 539-549

To link to this article: http://dx.doi.org/10.1080/10610278.2011.566614

Supramolecular Chemistry
Vol. 23, No. 7, July 2011, 539–549

Taylor & Francis
Taylor & Francis Group

Anthracene-based hetero bisamide chemosensor in fluorescence sensing of monocarboxylates over monocarboxylic acids

Kumaresh Ghosh* and Avik Ranjan Sarkar

Department of Chemistry, University of Kalyani, Kalyani, Nadia 741235, India

(*Received 7 December 2010; final version received 23 February 2011*)

A fluorescent chemosensor **1** with different amide moieties as recognition elements has been designed and synthesised. The recognition behaviour of the chemosensor towards various monocarboxylates and their conjugate acids has been evaluated. Although the sensor **1** shows significant quenching of emission of anthracene in CH_3CN, it shows an increase in emission in $CHCl_3$ containing 2% CH_3CN upon complexation of aliphatic monocarboxylates. Receptor **1** shows selectivity for acetate, propanoate and dihydrogen phosphate over the other anions studied under different conditions. The binding features have been established by ^1H NMR, UV–vis and fluorescence spectroscopic methods.

Keywords: monocarboxylate anion recognition; PET mechanism; anthracene-based receptor; unsymmetrical bisamide

Introduction

Molecular recognition of ionic substrates by designed artificial receptors is an area of keen interest (*1–3*). In this aspect, the important task is to design and construct a receptor that possesses size, shape and functional complementarities to a target substrate. As target substrates, carboxylates are important due to their biological significances (*4, 5*). In recent past, considerable efforts have been made to the development of fluorescent receptors of different architectures for both mono (*6–8*) and dicarboxylates (*9–12*), although the fluorescent receptors for monocarboxylate are rare (*13*). In designing such receptors, various hydrogen-bonding synthons such as urea/thiourea (*14, 15*) and guanidinium motifs (*16*) are well explored for carboxylate ion binding, and they are placed in the close vicinity of the different types of fluorophores. It is of important note that the use of 3-amidopyridinium motif for binding of carboxylate is less explored. Jeong and Cho reported the significance of unconventional C—H···O hydrogen bond in 3-amidopyridinium motif during complexation of carboxylate ions in polar solvent (*17*). Then, Steed and co-workers used this motif in several designs for complexation of spherical- and linear-shaped anions (*18*). In pursuit of developing fluorescent chemosensor, we addressed the use of this motif in selective sensing of anions such as dihydrogen phosphate, fluoride (*19*) and also dicarboxylates (*20, 21*) as their tetrabutylammonium salts. Based on inspiring results in using 3-amidopyridinium motif as a hydrogen-bonding motif for anions, we aimed at placing this motif in the vicinity of pyridine amide under the guidance of a flexible, semi-rigid spacer to generate a new hetero bisamide structure, which may serve as simple receptor for both carboxylate and carboxylic acid on the basis of binding complementarities. Under this situation, the pertinent query is whether such type of receptor molecule is capable of binding either carboxylate and carboxylic acid guests or any one of them with measurable selectivity. This has a strong relevance in enzyme model in which specificity in binding of a substrate is of prime importance. In an effort to understand this, we report here the design, synthesis and binding properties of **1** towards monocarboxylates and their conjugate acids in different solvents. The binding properties of the open cleft of **1** were also evaluated for tetrahedral-shaped anions such as $H_2PO_4^-$ and HSO_4^-.

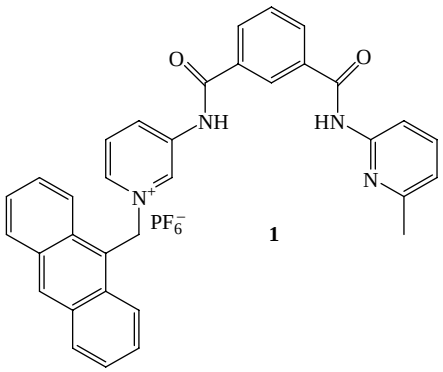

1

*Corresponding author. Email: ghosh_k2003@yahoo.co.in

ISSN 1061-0278 print/ISSN 1029-0478 online

DOI: 10.1080/10610278.2011.566614
http://www.informaworld.com

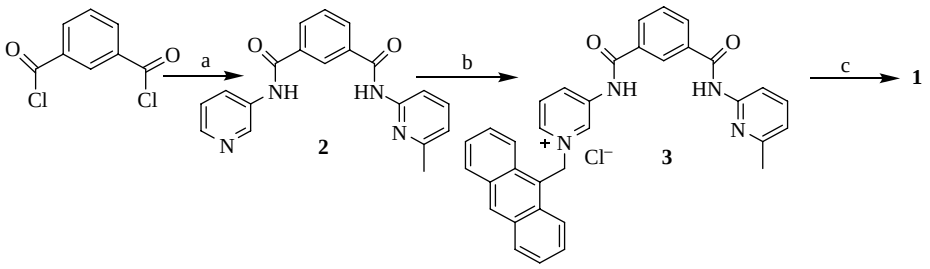

Scheme 1. (a) High dilution reaction with 2-amino-6-methylpyridine and 3-aminopyridine in the presence of Et_3N in dry CH_2Cl_2 (isolated yield: 18%); (b) 9-chloromethylanthracene, reflux in dry CH_3CN (isolated yield: 37%) and (c) NH_4PF_6, MeOH (yield: 62%).

Results and discussion

The receptor **1** was obtained according to Scheme 1. Initially, the hetero bisamide **2** was synthesised by high-dilution reaction of 3-aminopyridine and 2-amino-6-methylpyridine with isophthaloyl dichloride in dry CH_2Cl_2. Purification of the reaction mixture afforded **2** in 18% yield. Reaction of **2** with 9-chloromethylanthracene in dry CH_3CN under refluxing condition yielded the chloride salt **3**. It is to note that alkylation does not occur on to the methylated pyridine in spite of its better nucleophilicity. Such preferential alkylation on the nitrogen centre of 3-amidopyridine unit in **2** is presumably due to steric reason. However, anion exchange of the chloride salt **3** using NH_4PF_6 gave the receptor **1**.

To evaluate the hydrogen-bonding properties of the receptor **1** in solution, ^{1}H NMR, UV–vis and fluorescence experiments were performed in CH_3CN and $CHCl_3$ containing 2% CH_3CN solvents. The ability of the new receptor **1** to sense carboxylates and their conjugate acids was initially realised by fluorescence and UV–vis titrations. Figure 1 shows the changes in emission of receptor **1** ($c = 6.27 \times 10^{-5}$ M, excitation of anthracene fluorophore at 370 nm) upon addition of different monocarboxylic acids and their tetrabutylammonium salts such as acetate, propanoate, lactate, mandelate and benzoate (up to addition of 2 equivalent of guest).

Upon gradual addition of either carboxylic acid or carboxylate salt to the solution of **1** in CH_3CN, the monomer emission of **1** was quenched and the quenching was found to be significant only in the presence of carboxylate salts (Figure 1). This marked quenching effect on the emission of anthracene in **1** allows monocarboxylates (especially aliphatic) to be distinguished from monocarboxylic acids.

During titration, no peak at higher wavelength for excimer or exciplex was observed. It is also evident from Figure 1 that the extent of quenching of emission of **1** is also dependent on the steric feature of the monocarboxylates. Benzoate being steric in nature than the aliphatic monocarboxylates such as acetate, propanoate interacted poorly in the binding site and accordingly, perturbed the emission of **1** weakly. Due to similar reason, mandelate and lactate also exhibited weak interactions followed by moderate quenching of emission of anthracene in **1**. Figure 2 demonstrates the change in emission of **1** upon addition of $CH_3CH_2COO^-$ to the solution of **1**.

The quenching effect during complexation is attributed to a photo-induced electron transfer (PET) mechanism.

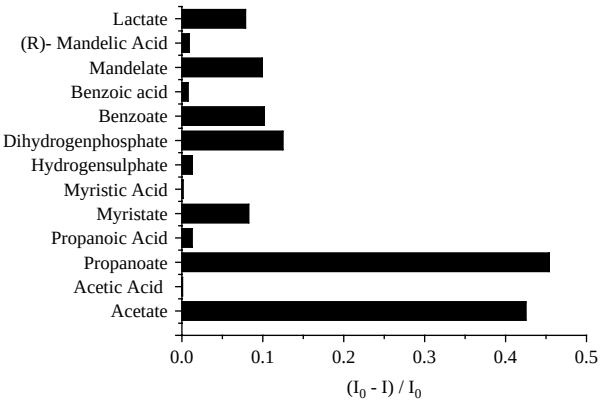

Figure 1. Fluorescence ratio $[(I_0 - I)/I_0]$ of receptor **1** ($c = 6.27 \times 10^{-5}$ M) at 412 nm upon addition of 2 equiv. of a particular tetrabutylammonium carboxylate and its acid in CH_3CN.

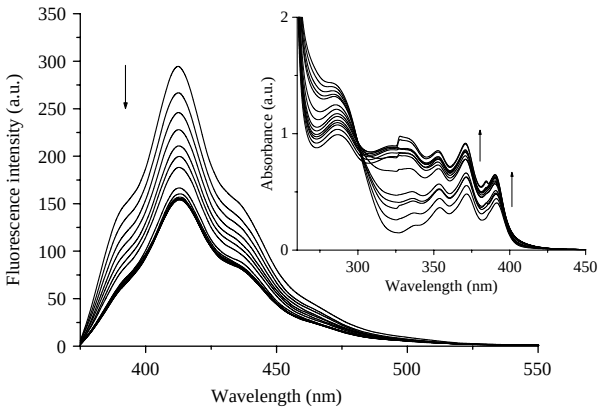

Figure 2. Change in emission of **1** ($c = 6.27 \times 10^{-5}$ M) in presence of increasing amounts of $CH_3CH_2COO^-$ in CH_3CN; inset: change in absorbance of **1** with $CH_3CH_2COO^-$ in CH_3CN.

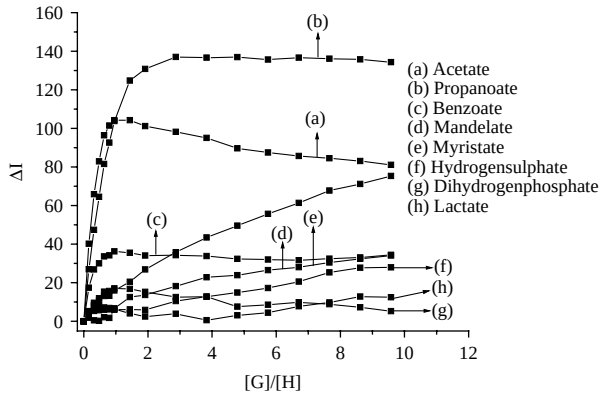

Figure 3. Plot of change in emission of **1** at 412 nm vs. the ratio of guest to host concentration in CH_3CN.

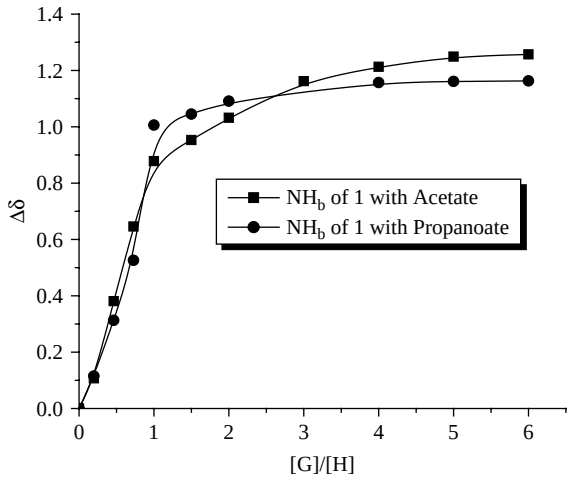

Figure 4. NMR titration curves for **1** with acetate and propanoate in CD_3CN.

In the interaction process, 1:1 stoichiometries of the complexes were realised from the break of titration curves at [G]/[H] = 1 in Figure 3. In this regard, for acetate, benzoate and dihydrogen phosphate, the titration curves continue to decrease after saturation suggesting that as greater excess of the guest anion is added, the 1:1 host–guest complex is disrupted and anions begin to bind individually to the pyridinium and pyridine amides, rather than in a cooperative manner. Thus, in principle, complexes of 1:1 and 2:1 (guest to host) stoichiometries may remain in equilibrium, in solution. Other anions except acetate, propanoate, benzoate and dihydrogen phosphate did not show this behaviour. Thus, this behaviour depends on the anions (*22a*) and also the concentration of the host and guest used at which the titration experiments are being monitored. It is of note that the downward running of the titration curves for AcO^- and $CH_3CH_2COO^-$ in Figure 3 was not observed when the titrations were carried out in ^{1}H NMR at the concentration range $\sim 10^{-3}$ M (Figure 4). The sharp break of the titration curves at [G]/[H] = 1 in Figure 4 indicates the formation of stable 1:1 complexes. In this context, it is mentionable that the titration of **1** with $H_2PO_4^-$ ion at $\sim 10^{-3}$ M was not possible due to precipitation. However, the downward running of the curve for $H_2PO_4^-$ ion in fluorescence titration is either due to the presence of excess $H_2PO_4^-$ that presumably causes deprotonation of the bound dihydrogen phosphate with the resultant formation of monohydrogen phosphate receptor complex as described by Gale et al. (*22b*) or due to partial decomplexation of $H_2PO_4^-$. Similarly, partial decomplexation of AcO^- and CH_3CH_2-COO^- at the concentration range 10^{-5} M cannot be ruled out. This is presumably another reason for downward running of the titration curves for AcO^- and CH_3CH_2-COO^- in Figure 3. However, Job plots (*22c*) for anions (AcO^-, $CH_3CH_2COO^-$, $C_6H_5COO^-$ and $H_2PO_4^-$) were additionally performed to confirm the exact stoichiometries of the complexes. Although downward running of the titration curves for AcO^-, $CH_3CH_2COO^-$, $C_6H_5COO^-$ and $H_2PO_4^-$ after [G]/[H] = 1 was noted in Figure 3, the inflection points at the mole fraction 0.5 in their Job plots corroborated 1:1 stoichiometry of the complexes. Figure 5, for example, represents the Job plot for **1** with $CH_3CH_2COO^-$ in which the stoichiometry is depicted as 1:1. For all the carboxylic acid guests, the titration curves were almost linear and thereby suggested weak interaction (see Supplementary Information, available online).

The fluorescence titration data were used to determine the association constants (*23*) of the complexes of **1** with the anionic guests. In the determination of the association constants, the stoichiometry of the complexes of all the anions was considered as 1:1. The results are summarised in Table 1. Binding constant values for acids were difficult to determine due to minimum change in emission upon

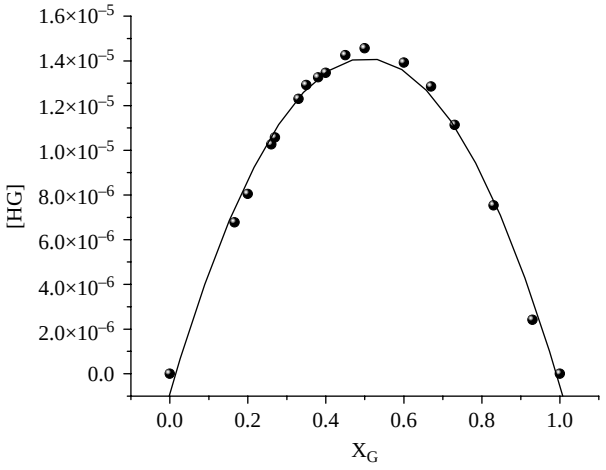

Figure 5. Fluorescence Job plot for **1** with tetrabutylammonium salt of propanoate at 372 nm in CH_3CN.

Table 1. Association constants (K_a) based on fluorescence and UV–vis methods in CH_3CN.

Guests	K_a (M^{-1})[a] (SD)	K_a (M^{-1})[b] (SD)
AcO^-	1.08×10^4 (0.11)	9.65×10^3 (0.25)
$CH_3CH_2COO^-$	1.25×10^4 (0.07)	1.34×10^4 (0.28)
Myristate		1.12×10^3 (0.56)
$C_6H_5COO^-$	–	1.34×10^3 (1.34)
(*R*)-Mandelate	6.08×10^3 (0.23)	–
$H_2PO_4^-$	–	3.83×10^3 (0.23)
HSO_4^-	–	–
Lactate	–	–

Notes: SD, standard deviation; dashes indicate that the association constants were not determined either due to minimal change or difficult to determine.
[a] Determined by fluorescence method at the wavelength of 412 nm.
[b] Determined by UV–vis method at the wavelength of 372 nm.

complexation (see Supplementary Information, available online). As given in Table 1, receptor **1** shows higher association constant values with acetate and propanoate compared to others. Long-chain myristate did not show any measurable change in emission of **1**. We presume that coiling nature of the long aliphatic chain probably introduces a steric clash into the isophthaloyl diamide core of **1** for which myristate exhibited weaker binding. Indeed, the preference in binding of AcO^- and $CH_3CH_2COO^-$ anions over $C_6H_5COO^-$ has the strong relevance in the distinction between aliphatic and aromatic monocarboxylates. The results further indicated the selectivity between carboxylates and carboxylic acids (see Figure 1), although the receptor **1** can provide binding complementarity to both kinds of guests. In spite of the binding complementarity of **1** with $H_2PO_4^-$, receptor **1** indicated almost no interaction in CH_3CN. Nonlinear least squares method (*24a*) was also adopted to check the reliability of binding constant values, and, for example, the values for AcO^- [$(K = 1.06 \pm 0.09) \times 10^4\,M^{-1}$] and $CH_3CH_2COO^-$ [$(K = 1.13 \pm 0.06) \times 10^4\,M^{-1}$] determined by fluorescence method were found to be comparable with the values found using linear curve fitting method (Table 1). ^1H NMR titration results for AcO^- and $CH_3CH_2COO^-$ were also used to determine the K_a (*24b*), and they were found to be $(1.78 \pm 0.35) \times 10^4\,M^{-1}$ and $(1.81 \pm 0.26) \times 10^4\,M^{-1}$, respectively.

The probable hydrogen-bonding structures of the complexes of **1** with carboxylate (**1A**, **1B** and **1C**), carboxylic acid (**1D**) and $H_2PO_4^-$ (**1E**) are shown in Figure 6 based on the hydrogen-bonding complementarities. Due to the flexible nature of **1**, cooperative binding mode **1A** for anions may remain in equilibrium with non-cooperative binding modes (**1B** and **1C**). This is true for carboxylic acids, $H_2PO_4^-$ and HSO_4^- also. Experimental findings and the previous report (*25a*) revealed that structures involving cooperative bindings (**1A**, **1D** and **1E**) dominate over the structures with non-cooperative bindings in the solution. In this context, binding-induced mutual activation of the binding sites and their cooperativities is recently well documented (*25b*). In ^1H NMR, downfield shifting of both the amide protons in **1** upon interaction with AcO^- and $CH_3CH_2COO^-$ further supported the cooperative mode of binding, i.e. mode **1A** (see Supplementary Information, available online).

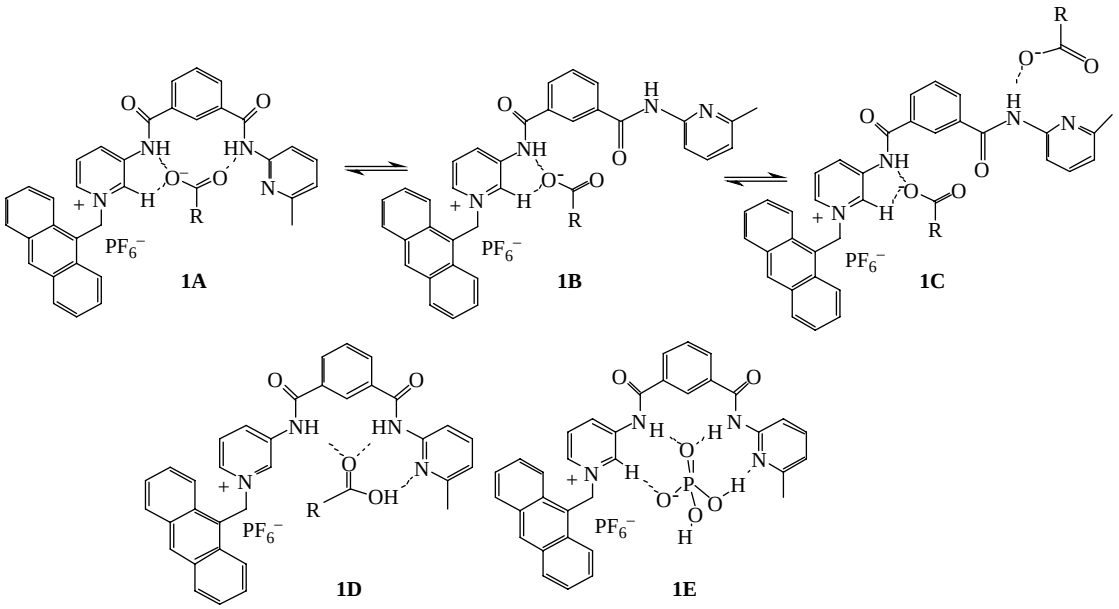

Figure 6. Possible modes of complexation of **1** with carboxylates, carboxylic acids and $H_2PO_4^-$.

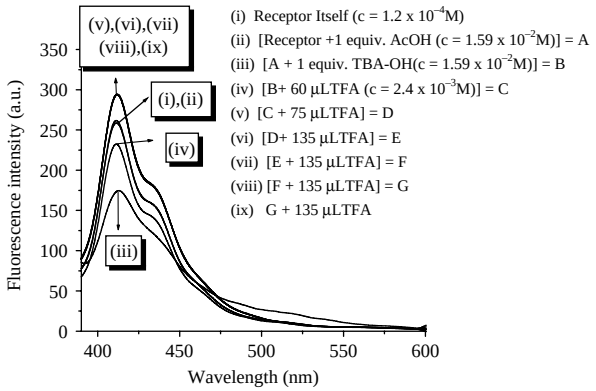

Figure 7. Emission profile for sensitivity of AcO^- over AcOH and the reversibility in the process.

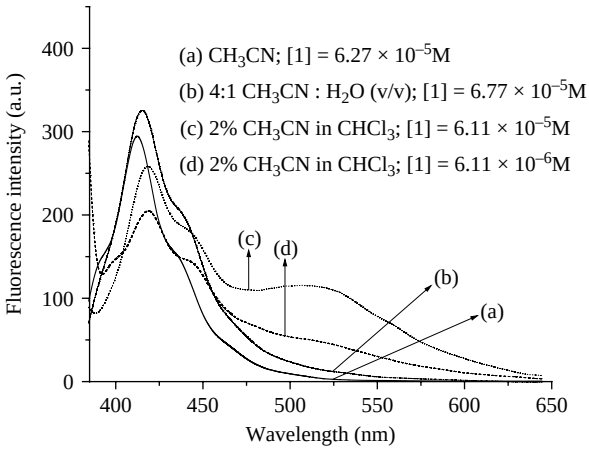

Figure 8. Emission spectra of **1** in different solvents ($\lambda_{ex} = 370$ nm).

The preference in the binding of carboxylate ion over carboxylic acid was realised by doing a control experiment in fluorescence. The emission intensity of **1** ($c = 1.20 \times 10^{-4}$ M) at 412 nm, which was almost unperturbed in the presence of equivalent amount of carboxylic acid, quenched to a considerable extent upon addition of equivalent amount of tetrabutylammonium hydroxide ($c = 1.59 \times 10^{-2}$ M). Upon addition of trifluoroacetic acid (TFA) ($c = 2.4 \times 10^{-3}$ M) to the resulting solution further caused an increase in emission and thereby indicated a reversibility in the process as well as a preference in binding towards monocarboxylate. Figure 7, for example, demonstrates this phenomenon with AcOH. It is mentionable that the individual addition of TFA and tetrabutylammonium hydroxide to the receptor solution of **1** caused negligible change in emission (see Supplementary Information, available online).

The simultaneous UV–vis experiments in CH_3CN upon addition of the same guests as mentioned in Table 1 showed minor changes in the absorbance of the anthracene peaks except for AcO^- and $CH_3CH_2COO^-$. For example, the change in absorbance of **1** upon gradual addition of $CH_3CH_2COO^-$ is represented in the inset of Figure 2. This further indicated the strong binding of $CH_3CH_2COO^-$. From the UV–vis titration in CH_3CN, the change in absorbance of the anthracene peak at 372 nm was used to determine the association constant (*21*) values (Table 1). The trend was similar to that of fluorescence. Even the binding constant values determined by nonlinear least square method (*24b*) using UV titration results [e.g. AcO^-: $K = (1.01 \pm 0.12) \times 10^4\,M^{-1}$; $CH_3CH_2COO^-$: $K = (1.14 \pm 0.08) \times 10^4\,M^{-1}$] were comparable with the values obtained by linear curve fitting method (Table 1). The stoichiometries of the complexes of **1** with the guests in the ground state were also 1:1 as confirmed by Job plots (see Supplementary Information, available online).

To increase the selectivity in binding for anions, we managed the solvent polarity. In $CHCl_3$ containing 2% CH_3CN, the receptor **1** showed an enhanced selectivity towards carboxylates and $H_2PO_4^-$ by exhibiting a different emission pattern. When **1** in $CHCl_3$ containing 2% CH_3CN was excited at 375 nm, it gave an emission at 416 nm along with a broad peak at 510 nm, which was attributed to the formation of intermolecular excimer between anthracene or exciplex between pyridine and excited anthracene (*26a*). The intensity of the peak at 510 nm is considerably less when the concentration of **1** is 6.11×10^{-6} M in $CHCl_3$ containing 2% CH_3CN. This suggested the self-association behaviour of **1** that results in the formation of excimer rather than exciplex (*26b*). In more polar solvents such as CH_3CN and CH_3CN/H_2O (4:1 v/v), this broad signal at 510 nm was no longer observed. Figure 8 demonstrates this comparative view.

However, upon addition of the carboxylates to the solution of **1** in $CHCl_3$ containing 2% CH_3CN, the monomer emission at 416 nm underwent minimum change

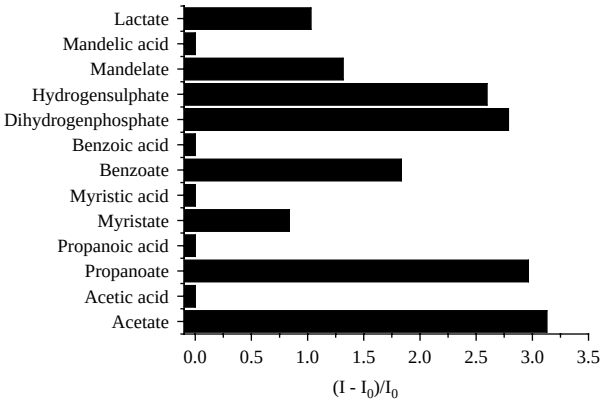

Figure 9. Fluorescence ratio $[(I - I_0)/I_0]$ of receptor **1** ($c = 6.11 \times 10^{-5}$ M) at 510 nm upon addition of 1 equiv. of a particular tetrabutylammonium salt of anions in $CHCl_3$ containing 2% CH_3CN.

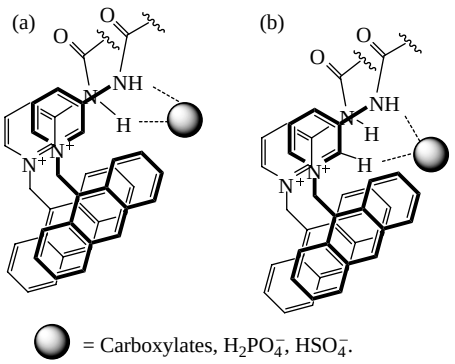

Figure 10. Proposed intermolecular binding interactions between **1** and anions involving (a) NH donors of pyridinium amides and (b) NH and CH donors of pyridinium amides.

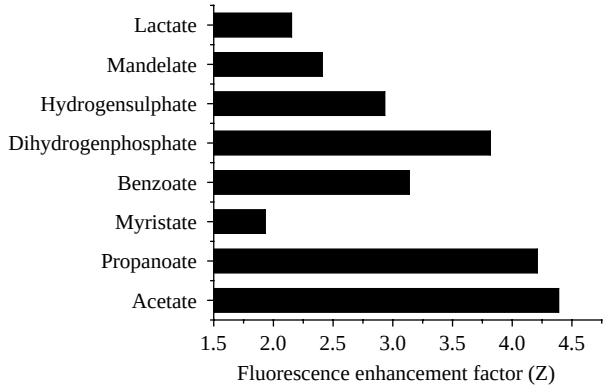

Figure 12. Fluorescence enhancement factor (*Z*) of **1** ($c = 6.11 \times 10^{-5}$ M) at 510 nm upon addition of 1 equiv. of a particular tetrabutylammonium salt of anions in $CHCl_3$ containing 2% CH_3CN.

up to 1:1 stoichiometry and then increased markedly when particular carboxylate was added in more amounts. The intensity of emission at 510 nm was gradually intensified on progression of the titration and it varied with nature of the carboxylate added. This suggested the persistence of strong intermolecular association of **1** in 2% CH_3CN in $CHCl_3$ even on complexation. The change in emission at 510 nm of **1** with the addition of different anions and carboxylic acids is displayed in Figure 9. It is evident from Figure 9 that the sensing ability of **1** in 2% CH_3CN in $CHCl_3$ is good to moderate for acetate, propanoate, dihydrogen phosphate and hydrogen sulphate. Carboxylic acids merely perturbed the emission (see Supplementary Information, available online). However, the gradual increase in intensity of the emission at 510 nm upon titration is explained by suggesting the different possible binding modes in Figure 10 that presumably originates from the guest-mediated intermolecular chelation (either in polymeric or discrete fashion) of the receptor **1** in solution (*26b*). Fluorescence Job plot confirmed 1:1 stoichiometry of the complexes in all cases (see Supplementary Information, available online).

Figure 11 displays the change in emission of **1** during complexation of acetate in $CHCl_3$ containing 2% CH_3CN. The complexation-induced increase in emission of **1** in $CHCl_3$ containing 2% CH_3CN is explained due to the inhibition of PET process. This is reversed to the case, observed in pure CH_3CN in which PET process was activated upon complexation. We believe that such different behaviours are essentially due to the different dispositions of MOs that take part in the PET process, in solvents of different polarities.

However, we also determined the fluorescence enhancement factor of **1** at the excimer wavelength (510 nm) in the presence of equivalent amount of each anion in 2% CH_3CN in $CHCl_3$. The increase in emission is a relative indicator of binding strength. Figure 12, in this regard, shows the plot of fluorescence enhancement factor (*Z*) (*26c*) in the presence of the different anions. From the plot, it is clearly understood that the response of the receptor towards acetate, propanoate and dihydrogen phosphate is significant.

Simultaneous UV titrations were conducted in $CHCl_3$ containing 2% CH_3CN and absorbance decreased on complexation (see Supplementary Information, available online). As representative, inset of Figure 11 shows the titration spectrum of **1** with acetate. The stoichiometries of the complexes of **1** with the anions in 2% CH_3CN in $CHCl_3$ were also 1:1 as established by Job plots and titration curves (see Supplementary Information, available online). Furthermore, during UV–vis titrations of **1** with all the monocarboxylates, clear isosbestic points were observed. This, indeed, indicated the formation of new species in solution.

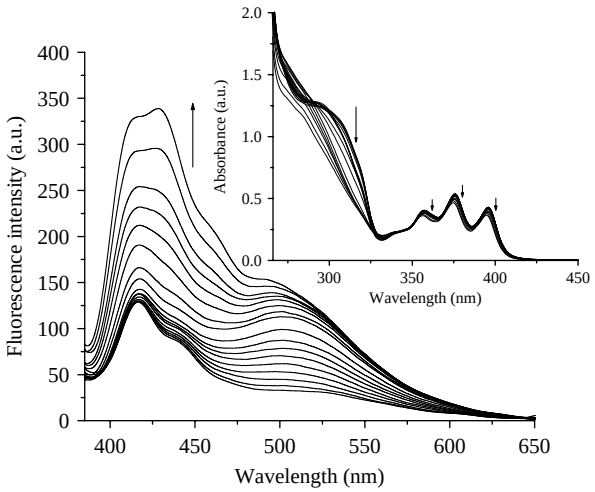

Figure 11. Change in emission of **1** ($c = 6.11 \times 10^{-5}$ M) in presence of increasing amount of CH_3COO^- in 2% CH_3CN in $CHCl_3$; inset: change in absorbance of **1** with CH_3COO^-.

Table 2. Association constants (K_a) based on fluorescence method in 2% CH_3CN in $CHCl_3$.

Guests	K_a (M^{-1})[a] (SD)	K_a (M^{-1})[b] (SD)
Acetate	1.16×10^4 (0.13)	1.33×10^4 (0.51)
Propanoate	1.04×10^4 (0.32)	8.85×10^3 (0.50)
Benzoate	3.02×10^3 (0.18)	1.03×10^3 (0.46)
Myristate	1.59×10^3 (0.63)	1.30×10^3 (0.56)
$H_2PO_4^-$	9.56×10^3 (0.10)	–
HSO_4^-	8.39×10^2 (0.04)	–
Lactate	1.32×10^3 (0.17)	–
Mandelate	1.96×10^3 (0.05)	1.45×10^3 (0.64)

Notes: SD, standard deviation; dashes indicate that the association constant was not determined either due to minimal change or due to greater percentage of error.
[a] Determined by fluorescence method at the wavelength of 510 nm.
[b] Determined by UV–vis method.

Binding constant values, determined (*23*) in 2% CH_3CN in $CHCl_3$ (Table 2), indicate that receptor has a clear cut selectivity for acetate, propanoate over benzoate and even myristate, a long-chain aliphatic monocarboxylate. Between dihydrogen phosphate and hydrogen sulphate, dihydrogen phosphate is complexed more strongly in the cavity.

In order to check the interaction properties of **1** in aqueous system, we performed the interaction of **1** in CH_3CN/H_2O (4:1 v/v) in the presence of the same guests but there was no measurable change in emission during the course of titrations (see Supplementary Information, available online).

The strong interactions of **1** with the carboxylates were also established from the change in ^1H NMR of **1** in the presence of equivalent amount of the guests. Due to insolubility of **1** in $CDCl_3$, we took ^1H NMR of **1** in d_6-DMSO and observed the change in chemical shift of the interacting protons in the presence of the guests. The amide protons H_a and H_b appeared at 11.22 and 10.83 ppm, respectively, and showed negligible downfield shift ($\Delta\delta = 0–0.3$ ppm for H_a and 0–0.07 ppm for H_b). This negligible change in chemical shift of the amide protons is attributed to the binding of DMSO (*26d*) into the open cavity. This was verified by replacing d_6-DMSO with CD_3CN, which did not interfere in the binding process. The amide protons H_a and H_b appeared at 10.08 and 9.34 ppm, respectively, in CD_3CN, and moved downfield measurably in the presence of aliphatic monocarboxylates. For example, Figure 13 shows the change in ^1H NMR of **1** in the presence of equivalent amounts of AcO^- and $CH_3CH_2COO^-$. Interestingly, during complexation *ortho* proton H_o of **1** was not found either due to broadening for strong complexation or due to deprotonation. The downfield shifting of the signal for H_o indicated the complexation-induced conformational change of **1** for which the H_o became close to the carboxylate ion for hydrogen bonding. In the event, the *para* proton H_p of **1** did not exhibit any measurable shift. Therefore, the possible hydrogen-bonding structures that may remain in equilibrium in solution are shown in Figure 14.

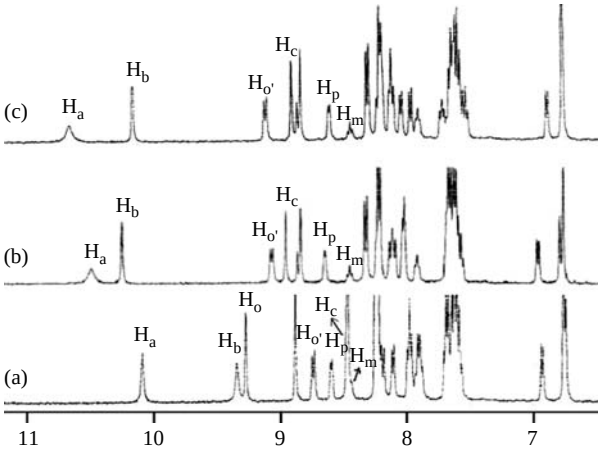

Figure 13. Partial ^1H NMR of (a) **1** ($c = 7.18 \times 10^{-3}$ M) and its 1:1 complexes with (b) $CH_3CH_2COO^-N^+Bu_4$ and (c) $CH^3COO^-\ N^+Bu_4$ in CD_3CN.

In addition, ^1H NMR of **1** with selected carboxylates and carboxylic acids were recorded in 2% CD_3CN in $CDCl_3$ to understand the recognition selectivity between carboxylates and carboxylic acids towards the cleft of **1** (see Supplementary Information, available online).

Theoretical observation

In order to understand the nature of orientation of the binding groups around isophthaloyl spacer, we performed DFT calculation using 6-31G* (*27*) basis set and the popular b3LYP (*28*) functional on the structure **1** as well as its complexes. Figure 15 shows the DFT optimised geometry of **1** showing the charges on the different atoms. From the DFT results, global electrophilicity index (ω; measure of electrophilic power to interact with

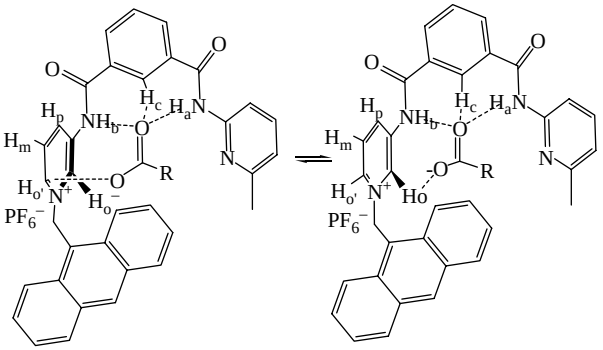

Figure 14. Suggested hydrogen-bonding structures of **1** with carboxylate in CD_3CN.

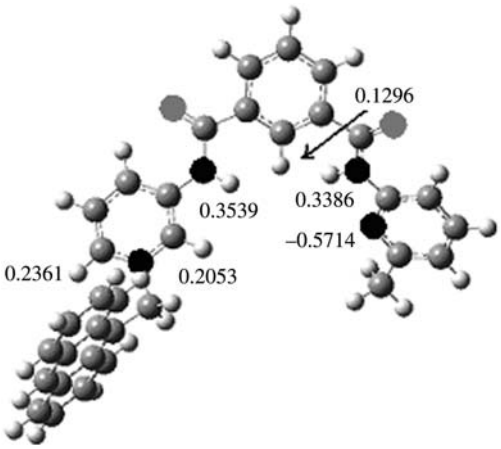

Figure 15. DFT-optimised geometry of **1** ($E = -1681.19$ a.u. and dipole moment $\mu = 3.42$ D).

nucleophiles; (*29a,b*)) of **1** was calculated, and it was found to be 0.3389. We also optimised the complexes of **1** with AcO^-, $CH_3CH_2COO^-$ and $H_2PO_4^-$ in gas phase. In this relation, Figure S20 (see Supplementary Information, available online) highlights the hydrogen-bonding schemes in which all the possible hydrogen-bond donors are intimately involved in complexation. Interestingly, the pyridine ring nitrogen is found to participate in the formation of unconventional C—H- - -N hydrogen bonds with carboxylate anions (Figure S20 of the Supplementary Information, available online) and conventional O—H- - -N bond with $H_2PO_4^-$ (Figure S20 of the Supplementary Information, available online). In the complexes, the pyridinium *ortho* proton (H_o) is also involved in hydrogen bonding with the anions and overall supports the experimental findings.

Conclusion

In conclusion, a simple hetero bisamide receptor containing anthracene moiety in a selective position has been synthesised as a fluorescent chemosensor for aliphatic monocarboxylates. The receptor shows selective binding of monocarboxylates over their conjugate acids in spite of having binding complementarity to both carboxylate and carboxylic acid. The results indicate that the open cleft of the receptor can distinguish the aliphatic carboxylates such as AcO^-, $CH_3CH_2COO^-$ from their acid analogues and also other anions studied by exhibiting significant change in emission in different solvent combinations. Analysis of the results shows that in 2% CH_3CN in $CHCl_3$ is a better choice of solvent to attain greater selectivity for sensing anions, especially short-chain aliphatic monocarboxylates AcO^-, $CH_3CH_2COO^-$ and also tetrahedral-shaped anion $H_2PO_4^-$ from HSO_4^-. The high affinity of such simple receptor for anion is due to its significant global electrophilic character as calculated theoretically. The hydrogen bonding (N—H- - -O and C—H- - -O) and charge–charge interactions as a whole contribute to stabilise the complex of carboxylates over the carboxylic acids, where the charge–charge interaction is absent. In this regard, although it is obvious that the charged guest has a preference over the neutral one because of electrostatic reason, this systematic study in the present report is quite meaningful to understand the hydrogen-bonding behaviour as well as sensing property of a simple hetero bisamide receptor. The sensing ability of this hetero bisamide receptor is dependent on the polarity of the solvent used, and in the present case $CHCl_3$ containing 2% CH_3CN is the better choice in reporting the recognition and sensing properties successfully for a wide range of anions. Further progress in this direction is underway in our laboratory.

Experimental

Synthesis

N*1-(6-methylpyridin-2-yl)*-N*3-(pyridin-3-yl) isophthalamide (2)*

The unsymmetrical hetero bisamide **2** was obtained by simultaneous dropwise addition of 2-amino-6-methylpyridine (0.532 g, 4.93 mmol, dissolved in 20 ml dry $CH_2—Cl_2$) and 3-aminopyridine (0.463 g, 4.93 mmol, dissolved in 20 ml dry $CH_2—Cl_2$) to the solution of isophthaloyl diacid chloride (1 g, 4.92 mmol) in dry CH_2Cl_2 (30 ml) at high dilution condition under nitrogen atmosphere. Triethylamine (4.92 mmol) was added in each amine solution during the reaction. After completion of addition of the amines, the reaction mixture was stirred overnight. The progress of the reaction was monitored by thin layer chromatography (TLC). After completion of the reaction, the solvent was evaporated and the residual mass was extracted with $CHCl_3/CH_3OH$ mixture ($CHCl_3$:CH_3OH = 4:1; 3 × 20 ml). The organic extract was next washed with $NaHCO_3$ solution (3 × 15 ml) and dried over anhydrous Na_2SO_4. The solvent was removed under vacuum, and the residual mass was purified by silica gel column chromatography using 4:1 ethyl acetate:petroleum ether as eluent to afford the compound **2** (304 mg, 18% yield, mp 192°C). ^{1}H NMR (d_6-DMSO, 400 MHz): 10.49 (s, NH, 1H), 9.99 (s, NH, 1H), 9.06 (s, 1H), 8.73 (s, 1H), 8.50 (d, 1H, $J = 8$ Hz), 8.34 (d, 2H, $J = 8$ Hz), 8.19 (d, 1H, $J = 1.2$ Hz), 8.17 (d, 1H, $J = 1.2$ Hz), 7.81 (t, 1H, $J = 8$ Hz), 7.60 (t, 1H, $J = 7.8$ Hz), 7.38–7.35 (m, 1H), 7.04 (d, 1H, $J = 8$ Hz) and 2.56 (s, 3H). ^{13}C NMR (d_6-DMSO, 125 MHz): 166.7, 165.4, 156.7, 151.4, 144.8, 142.1, 138.5, 135.7, 134.4, 133.3, 131.3, 130, 129.1, 128.7, 127.4, 123.6, 119.2, 111.6 and 23.6. FTIR: ν cm^{-1} (KBr): 3395, 2959, 2918, 2849, 1675, 1660, 1544 and 1458. *m/z*

(ES +): 333.4 $(M + H)^+$, 225.3 and 167.1. Analysis calculated for $C_{19}H_{16}N_4O_2$: C 68.66, H 4.85 and N 16.86. Found: C 68.52, H 4.91 and N 16.71.

*1-(Anthracen-9-ylmethyl)-3-(3-(6-methylpyridin-2-ylcarbamoyl)benzamido)pyridinium hexafluorophosphate (V) (**1**)*

Compound **2** (0.08 g, 0.26 mmol) was treated with 9-chloromethyl anthracene (0.07 g, 0.32 mmol) in dry CH_3CN (30 ml), and the reaction mixture was refluxed for 48 h to afford the chloride salt **3** (60 mg, 37% yield). The compound **3** (0.055 g, 0.098 mmol) in MeOH (20 ml) was subsequently treated with aqueous NH_4PF_6 solution to carry out the anion exchange reaction. After heating with stirring of the solution for 20 min, precipitate appeared. Filtration of the precipitate followed by thorough washing with ether afforded the receptor **1** in 67% yield (42 mg, mp 158°C). ^{1}H NMR (d_6-DMSO, 400 MHz): 11.23 (s, NH, 1H), 10.85 (s, NH, 1H), 9.33 (s, 1H), 8.96 (s, 1H), 8.81 (d, 1H, $J = 8$ Hz), 8.75 (d, 1H, $J = 8$ Hz), 8.46 (d, 2H, $J = 8$ Hz), 8.43 (s, 1H), 8.27 (d, 2H, $J = 8$ Hz), 8.24 (d, 1H, $J = 8$ Hz), 8.13 (t, 1H, $J = 8$ Hz), 8.04 (d, 1H, $J = 8$ Hz), 8.00 (d, 1H, $J = 8$ Hz), 7.76–7.62 (m, 6H), 7.05 (d, 1H, $J = 8$ Hz), 7.01 (s, 2H) and 2.45 (s, 3H). ^{13}C NMR (d_6-DMSO, 125 MHz): 165.8, 165.0, 156.5, 151.2, 139.6, 138.9, 138.4, 135.2, 134.4, 134.1, 133.1, 131.7, 131.4, 131.1, 131.0, 129.5, 128.7 (1C unresolved), 128.3, 128.2, 127.5, 125.7, 123.1, 121.6, 119.2, 111.5, 56.4 and 23.4. FTIR: $\nu\,cm^{-1}$ (KBr): 3384, 2951, 2922, 2853, 1681, 1673, 1548 and 1454. *m/z* (ES +): 669.4 $(M + H)^+$, 523.4 $[(M - PF6)]^+$, 333.5 and 225.2. Analysis calculated for $C_{34}H_{27}F_6N_4O_2P$: C 61.08, H 4.07 and N 8.38. Found: C 60.92, H 4.16 and N 8.24.

General procedure for fluorescence and UV–vis titrations

Stock solutions of the receptor were prepared in different solvents such as CH_3CN and $CHCl_3$ containing 2% CH_3CN in the concentration range $\sim 10^{-5}$ M. A sample of 2.5 ml receptor solution was taken in the cuvette. Stock solutions of guests in the concentration range $\sim 10^{-3}$ M were prepared in the same solvents, and were individually added in different amounts to the receptor solution. For fluorescence, the solution was irradiated at the excitation wavelength of 370 nm maintaining the excitation and emission slits 12 and 10, respectively. Upon addition of guests, the change in emission of the receptor was noted.

Same stock solutions for receptor and guests were used to perform the UV–vis titration experiment. Guest solution was successively added in different amounts to the receptor solution (2.5 ml) taken in the cuvette, and the absorption spectra were recorded. Both fluorescence and UV–vis titration experiments were carried out at 25°C. All the experiments were repeated thrice to check the reproducibility.

General method for NMR titration

Stock solutions of host ($c = 7.18 \times 10^{-3}$ M) and guests ($c = 4.79 \times 10^{-2}$ M for AcO^- and 4.54×10^{-2} M for $CH_3CH_2COO^-$) were made in CD_3CN. In each titration, 0.5 ml of the host was transferred to an NMR tube, and the spectrum was collected. Then, guest solution was added to the host solution in different amounts and ^{1}H NMR spectra were collected. The chemical shifts of the resonances corresponding to the amides of the host **1** were noted and used in the determination of binding constant values.

Method for Job plot

In this method, the stoichiometry of the complexes was determined using the continuous variation method (*22c*), and the solutions of host and guests of equal concentrations were prepared using the solvents used in the experiment. Then host and guest solutions were mixed in different proportions maintaining a total volume of 3 ml of the mixture. All the prepared solutions were kept for 1 h with occasional shaking at room temperature. Then, emission and absorbance of the solutions of different compositions were recorded. The concentration of the complex, i.e. [HG] was calculated using the equation $[HG] = \Delta I/I_0 \times [H]$ or $[HG] = \Delta A/A_0 \times [H]$, where $\Delta I/I_0$ and $\Delta A/A_0$ indicate the relative emission and absorbance intensities and [H] corresponds the concentration of pure host. Mole fraction of the host (X_H) was plotted against concentration of the complex [HG]. In the plot, the mole fraction of the host at which the concentration of the host–guest complex concentration [HG] is maximum gives the stoichiometry of the complex.

Determination of binding constant

The measured relative fluorescence intensities $[I_0/(I_0 - I)]$ as a function of the inverse of guest concentrations were plotted to ascertain the binding constant values. The ratio of the intercept to the slope gave the binding constant (K_a) values (*22*). In the similar way, using the absorbance data, the binding constant values were determined from the plot of $[A_0/(A_0 - A)]$ versus 1/[G]. For the determination of the binding constant values for AcO^-, $CH_3CH_2CO_2^-$, $C_6H_5CO_2^-$ and $H_2PO_4^-$, we considered the emission and absorbance data up to the addition of 1 equivalent amount of the guest to the receptor solution. NMR titration results for AcO^- and $CH_3CH_2CO_2^-$ were used to evaluate the binding constant values through nonlinear curve fit using

Origin 6.0. The working formula (*23*) used for this was

$$\delta_{Obs} = (\delta_C - \delta_H)(\{(1 + [G]/[H] + 1/K_a[H])/2\} - \{(1 + [G]/[H] + 1/K_a[H])^2/4[G]/[H]\}^{1/2}) + \delta_H.$$

Computational study

Structure **1** was optimised in gas phase at DFT [6-31G* (*27*) and B3LYP (*28*)] level, individually and in presence of acetate, propanoate and dihydrogen phosphate anions. The Gaussian-03 package (*27*) was used for the calculations. For the structure **1**, the global electrophilicity index (ω; measure of electrophilic power to interact with the nucleophiles; (*29a,b*)) was determined by the equation: $\omega = \chi^2/2\eta$, where χ and η are the electronegativity and hardness, respectively. Electronegativity (χ) (*30*) and the hardness (η) (*31*) were obtained from the relations $\chi = (E_{HOMO} + E_{LUMO})/2$ and $\eta = E_{LUMO} - E_{HOMO}$, where E_{HOMO} and E_{LUMO} are the energies of the highest occupied and lowest unoccupied molecular orbitals, respectively.

Supporting information

Change in emission and absorption of **1** with selected guests (anions and carboxylic acids) in CH_3CN and in 2% CH_3CN in $CHCl_3$, Job plots for **1** with the guests in CH_3CN and in 2% CH_3CN in $CHCl_3$, selected binding constant curves, change in emission of **1** in the presence of propanoate in CH_3CN/H_2O (4:1 v/v), DFT-optimised geometry of the complex of **1** with $H_2PO_4^-$, ^1H NMR studies, spectral data of **1** and **2**.

Acknowledgements

K.G. expresses his deep sense of gratitude to Professor Uday Maitra, IISC, Bangalore, for his valuable suggestions. We thank CSIR, New Delhi, India, for financial support. ARS thanks University of Kalyani, West Bengal, India, for a university research fellowship.

References

(1) (a) Schmidtchen, F.P.; Berger, M. *Chem. Rev.* **1997**, *97*, 1609–1646. (b) Gavette, J.V.; McGrath, J.M.; Spuches, A.M.; Sargent, A.L.; Allen, W.E. *J. Org. Chem.* **2009**, *74*, 3706–3710.
(2) Martinez-Manez, R.; Sancenon, F. *Chem. Rev.* **2003**, *103*, 4419–4476.
(3) Kondo, I.S.; Hiroka, Y.; Kurmatani, N.; Yano, Y. *Chem. Commun.* **2005**, 1720–1722.
(4) Voet, D.; Voet, J.G. *Biochemistry*; 2nd ed. Wiley: New York, 1995.
(5) Kral, V.; Andrievsky, A.; Sessler, J.L. *J. Am. Chem. Soc.* **1995**, *117*, 2953–2954.
(6) Gunnlaugsson, T.; Davis, A.P.; Glynn, M. *Chem. Commun.* **2001**, 2556–2557.
(7) Gunnlaugsson, T.; Davis, A.P.; Hussey, G.M.; Tierney, J.; Glynn, M. *Org. Biomol. Chem.* **2004**, *2*, 1856–1863.
(8) (a) Gunnlaugsson, T.; Glynn, M.; Tocci, G.M.; Kruger, P.E.; Peffer, F.M. *Coord. Chem. Rev.* **2006**, *250*, 3094–3117. (b) Gil, S. *Tetrahedron Lett.* **2006**, *47*, 6561–6564.
(9) Gunnlaugsson, T.; Davis, A.P.; O'Brien, E.; Glynn, M. *Org. Lett.* **2002**, *4*, 2449–2452, and reference cited therein.
(10) Qin, D.-B.; Xu, F.-B.; Wan, X.-J.; Zhao, Y.-J.; Zhang, Z.-Z. *Tetrahedron Lett.* **2006**, *47*, 5641–5643.
(11) Tseng, Y.-P.; Tu, G.-M.; Lin, C.-H.; Chang, C.-T.; Lin, C.-Y.; Yen, Y.-P. *Org. Biomol. Chem.* **2007**, *5*, 3592–3598, and reference cited therein.
(12) Costero, A.M.; Gil, S.; Parra, M.; Allouni, Z.; Lakhmiri, R.; Atlamsani, A. *J. Incl. Phenom. Macrocycl. Chem.* **2008**, *62*, 203–207.
(13) (a) Goswami, S.; Hazra, A.; Chakrabarty, R.; Fun, H.-K. *Organic Lett.* **2009**, *11*, 4350–4353. (b) Goswami, S.; Jana, S.; Chakrabarty, R.; Fun, H.-K. *Supramol. Chem.* **2010**, *20*, 145–148. (c) Goswami, S.; Hazra, A.; Das, M.K. *Tetrahedron Lett.* **2010**, *51*, 3320–3323. (d) Goswami, S.; Sen, D. *Tetrahedron Lett.* **2010**, *51*, 6207–6208.
(14) Blondean, P.; Benet-Buchholz, J.; De Mendoza, J. *New. J. Chem.* **2007**, *31*, 736–740.
(15) Ghosh, K.; Adhikari, S. *Tetrahedron Lett.* **2006**, *47*, 8156–8169, and reference cited therein.
(16) Lee, N.H.; Sing, N.J.; Kim, S.K.; Kwon, Y.; Kim, Y.Y.; Kim, K.S.; Yoon, J. *Tetrahedron Lett.* **2007**, *48*, 169–172.
(17) Jeong, K.-S.; Cho, Y.L. *Tetrahedron Lett.* **1997**, *38*, 3279–3282.
(18) Wallance, K.J.; Belcher, W.J.; Turner, D.R.; Syed, K.F.; Steed, J.W. *J. Am. Chem. Soc.* **2003**, *125*, 9699–9715.
(19) Ghosh, K.; Sarkar, A.R.; Masanta, G. *Tetrahedron Lett.* **2007**, *48*, 8725–8729.
(20) Ghosh, K.; Sarkar, A.R. *Tetrahedron Lett.* **2009**, *50*, 85–88.
(21) Ghosh, K.; Masanta, G.; Chattopadhyay, A.P. *Tetrahedron Lett.* **2007**, *48*, 6129–6132.
(22) (a) Turner, D.R.; Paterson, M.J.; Steed, J.W. *J. Org. Chem.* **2006**, *71*, 1598–1608. (b) Gale, P.A.; Hiscock, J.R.; Moore, S.J.; Caltagirone, C.; Hursthouse, M.B.; Light, M.E. *Chem. Asian J.* **2009**, *5*, 555–561. (c) Job, P. *Ann. Chim.* **1928**, *9*, 113–203.
(23) Chou, P.T.; Wu, G.R.; Wei, C.Y.; Cheng, C.C.; Chang, C.P.; Hung, F.T. *J. Phys. Chem. B* **2000**, *104*, 7818–7829.
(24) (a) Valeur, B.; Pouget, J.; Bourson, J.; Kaschke, M.; Eensting, N.P. *J. Phys. Chem.* **1992**, *96*, 6545–6549. (b) Fielding, L. *Tetrahedron* **2000**, *56*, 6151–6170.
(25) (a) Goswami, S.P.; Ghosh, K.; Dasgupta, S. *Tetrahedron* **1996**, *52*, 12223–12232. (b) dos Santos, C.M.G.; McCabe, T.; Watson, G.W.; Kruger, P.E.; Gunnlaugsson, T. *J. Org. Chem.* **2008**, *73*, 9235–9244.
(26) (a) Xu, Z.; Kim, S.; Lee, K.-H.; Yoon, J. *Tetrahedron Lett.* **2007**, *48*, 3797–3800. (b) Nishizawa, S.; Kato, Y.; Teramae, N. *J. Am. Chem. Soc.* **1999**, *121*, 9463–9464. (c) Fluorescence enhancement factor (Z) was calculated based on the equation $Z=(F/F_0)$ $[(V_0 + V)/V_0]$ where F=observed fluorescence, F_0=fluorescence of sample before guest addition, V_0=volume before addition, V=volume addition. (d) Kovalchuk, A.; Bricks, J.; Reck, L.G.; Rurack, K.; Schulz, B.; Szumnac, A.; Weißhoff, H. *Chem. Commun.* **2004**, 1946–1947.
(27) (a) Gaussian 03, Revision C.01, Frisch, M.J.; Trucks, G.W.; Schlegel, H.B.; Scuseria, G.E.; Robb, M.A.; Cheeseman, J.R.; Montgomery, J.A.; Vreven, Jr., T.; Kudin, K.N.;

Burant, J.C.; Millam, J.M.; Iyengar, S.S.; Tomasi, J.; Barone, V.; Mennucci, B.; Cossi, M.; Scalmani, G.; Rega, N.; Petersson, G.A.; Nakatsuji, H.; Hada, M.; Ehara, M.; Toyota, K.; Fukuda, R.; Hasegawa, J.; Ishida, M.; Nakajima, T.; Honda, Y.; Kitao, O.; Nakai, H.; Klene, M.; Li, X.; Knox, J.E.; Hratchian, H.P.; Cross, J.B.; Adamo, C.; Jaramillo, J.; Gomperts, R.; Stratmann, R.E.; Yazyev, O.; Austin, A.J.; Cammi, R.; Pomelli, C.; Ochterski, J.W.; Ayala, P.Y.; Morokuma, K.; Voth, G.A.; Salvador, P.; Dannenberg, J.J.; Zakrzewski, V.G.; Dapprich, S.; Daniels, A.D.; Strain, M.C.; Farkas, O.; Malick, D.K.; Rabuck, A.D.; Raghavachari, K.; Foresman, J.B.; Ortiz, J.V.; Cui, Q.; Baboul, A.G.; Clifford, S.; Cioslowski, J.; Stefanov, B.B.; Liu, G.; Liashenko, A.; Piskorz, P.; Komaromi, I.; Martin, R.L.; Fox, D.J.; Keith, T.; Al-Laham, M.A.; Peng, C.Y.; Nanayakkara, A.; Challacombe, M.; Gill, P.M.W.; Johnson, B.; Chen, W.; Wong, M.W.; Gonzalez, C.; Pople, J.A. Gaussian, Inc: Wallingford, CT, 2004. (b) Schmidt, M.W.; Baldridge, K.K.; Boatz, J.A.; Elbert, S.T.; Gordon, M.S. *J. Comput. Chem.* **1993**, *14*, 1347–1363. (c) Podolyan, Y.; Leszczynski, J. *Int. J. Quantum Chem.* **2009**, *109*, 8–16. (d) Krishnan, R.; Binkeley, J.S.; Seeger, R.; Pople, J.A. *J. Chem. Phys.* **1980**, *72*, 650–654.

(28) (a) Becke, A.D. *J. Chem. Phys.* **1993**, *98*, 5648–5652. (b) Stephens, P.J.; Devlin, F.J.; Chabalowski, C.F.; Frisch, M.J. *J. Phys. Chem.* **1994**, *98*, 11623–11627.

(29) (a) Chattaraj, P.K.; Sarkar, U.; Roy, D.R. *Chem. Rev.* **2006**, *106*, 2065–2091. (b) Parr, R.G.; Szentpaly, L.V.; Liu, S. *J. Am. Chem. Soc.* **1999**, *121*, 1922–1924.

(30) Pearson, R.G. *Inorg. Chem.* **1988**, *27*, 734–740.

(31) Koopmans, T.A. *Physica* **1933**, *1*, 104–113.